DEFINITION OF THE EQUIVALENT SHEAR STRESS, BASED ON THE ELLIPSOID SIMPLIFIED MODEL FOR DETERMINATION OF THE MULTIAXIAL FATIGUE LIMIT

Lucival Malcher, malcher@unb.br
José Carlos Balthazar, jcbalthazar@unb.br
University of Brasilia
Department of Mechanical Engineering
Brasília – DF – Brazil

Abstract. *In the last fifteen years, innumerable researchers come considering models in the direction to contemplate the influence of the out-of-phase in the fatigue properties of materials and mechanical components. Out-of-phase multiaxial loadings cause a reduction in the fatigue limit. According to the stress invariant approach, the maximum hydrostatic stress and the equivalent shear stress amplitude, are the parameters that govern the initiation process of crack fatigue in multiaxial conditions. Thus, the attainment of these parameters, became a challenge for designers and researchers, in the direction to correct design and safe operational life of many structural components. In such a way, in this work, one searched to develop a simplified model, in the definition of the equivalent shear stress amplitude, for determination of the multiaxial fatigue limit, based in the stress invariant approach. Finally, a comparison of the results presented with the other available models in literature became.*

Keywords*: multiaxial fatigue limit, out-of-phase loading, stress invariant, ellipsoid simplified model.*

1. INTRODUCTION

Many mechanical components, as shafts, torsion bars, pressure vessels, aeronautical components among others, are frequently subjected to cyclically combined bending/torsion loading producing multiaxial stress states that can initiate fatigue cracks. The fatigue process under such states of stresses is known as multiaxial fatigue and its consideration is of basic importance for the correct design, life assessment and operational reliability of components submitted to combined loadings.

Although many important advances on multiaxial fatigue have been made, large factors of safety are still being employed to guard against premature fatigue failures. Thus, the estimation of fatigue strength of a component under combined bending/torsion loading is fundamental for correct design and safe operational life of structural components under such loading conditions. The assessment of fatigue behaviour under multiaxial stress states stems generally from three different approaches. Under the equivalent stress or strain methods an equivalent uniaxial stress which would produce the same fatigue life as the multiaxial cyclic stress states is defined and compared to a fatigue limit, which can be obtained from reverse bending tests. The critical planes approach considers a critical plane where the fatigue strength should be assessed, determined by maximising the amplitudes and/or values of some stressor strain component. The plastic work and energy methods try to correlate fatigue life to crack initiation to the plastic work, done in each cycle.The application of such theories depends on the stress-strain response of the material under multiaxial loading. The applicability of all these methods requires a number of parameters to be determined experimentally.

Despite the critical plane approach have had a great acceptance in reason of the appealing physical interpretation of the multiaxial fatigue behaviour in terms of the cracking process, the definition of critical plane is still matter of some controversy, as can be inferred from the definitions for the most probable planes for crack growth presented by different authors.

The criteria proposed by Crossland, Sines, Kakuno-Kawada and the approaches of Dang Van et al, Deperrois, Marin, Duprat et al, Bin Li et al and Mamiya & Araújo for determination of the amplitude equivalent shear main multiaxial fatigue strength criteria are reviewed. These methods are a combination of the critical plane method and the equivalent stress methods as they establish inside the deviatory plan a shear stress equivalent to the applied multiaxial stresses. According Papadopoulos (1992), these methods give a good estimation for in-phase loadings. However, for out-of-phase loading the principal stress and strain axis change direction along the time and it has long been recognised that changing of the principal stress directions influences fatigue phenomena.

In the present work, a model to predict fatigue strength under combined bending/torsion loading based on stress invariant method is proposed. This model was derived combining the models proposed by Duprat et al (1997) and by Bin Li et al (2000), determining the minimum elipsoid contaning the path of the deviatory tensor using some parameters of the Duprat model to calculate the equivalent shear stress amplitude.

2. THE STRESS INVARIANT METHODS

The invariant stress approach is based on the invariants of the stress tensor and/or its deviator tensor. The basic idea is to directly relate the fatigue strength with the second invariant of the stress deviator and first invariant of the stress (3 times the hydrostatic stress). The initiation of a fatigue crack under cyclic loading would be predicted when the left side of the equation below gets bigger than the right side:

$$\sqrt{J_{2,a}} + k(N)\sigma_H \leq \lambda(N) \tag{1}$$

where: $\sqrt{J_{2,a}}$ is the equivalent shear stress amplitude, σ_H is the hydrostatic stress and $k(N)$ and $\lambda(N)$ are parameters to be experimentally determined.

Some models which use only the first invariant of the stress tensor and the second invariant the deviator tensor can be regarded as a combination of the equivalent stress approach, as it uses a shear stress equivalent to the multiaxial applied stresses, and the critical plane approach, as it searches for the maximum values of their parameters in a plan with the greatest intersection with the path of the deviatory stress tensor. The models of Sines (1955), Crossland (1956) and Kakuno-Kawada (1979) can be also be classified in this category are good representatives of this kind of approach.

Sines (1955) criterion is mathematically expressed as:

$$\sqrt{J_{2,a}} + k\sigma_{H,mean} \leq \lambda \tag{2}$$

where $\sqrt{J_{2,a}}$ is the equivalent shear stress amplitude and $\sigma_{H,mean}$ is the mean hydrostatic stress. The parameters k and λ are material constants, which can be obtained from two simple fatigue tests: the repeated bending limit f0 (σa = σm = f0) and the fully reversed torsion limit t-1 (τa = t-1 , τm = 0).

$$k = \left(\frac{3t_{-1}}{f_0}\right) - \sqrt{3} \;\; ; \;\; \lambda = t_{-1} \tag{3}$$

Instead of the mean hydrostatic stress, the Crossland (1956) criterion considers the influence of the maximum hydrostatic stress, $\sigma_{H,\max}$:

$$\sqrt{J_{2,a}} + k\sigma_{H,\max} \leq \lambda \tag{4}$$

The parameters k and λ can be also obtained as Sines criterion

Kakuno and Kawada (1979) suggested that the contribution of the invariant of the stress deviator and the hydrostatic stress should be different:

$$\sqrt{J_{2,a}} + k\sigma_{H,a} + \lambda\sigma_{H,m} \leq \mu \tag{5}$$

where the parameters k, λ e μ should be determined from three uniaxial fatigue limits: f_0, t_{-1} e f_{-1} (repeated bending, fully reversed torsion, fully reversed bending). Thus,

$$k = \left(\frac{3t_{-1}}{f_{-1}}\right) - \sqrt{3} \;\; ; \;\; \lambda = \left(\frac{3t_{-1}}{f_0}\right) - \sqrt{3} \;\; ; \;\; \mu = t_{-1} \tag{6}$$

For these criteria, failure will occur when the left side of the equation gets greater than the right side.

2.1. The Equivalent Shear Stress Amplitude

The basic difference in the application of the models based on the invariants of the stress tensors, as the models of Sines (1955), Crossland (1956) and Kakuno-Kawada (1979), is the value, mean or maximum, of the hydrostatic stress σ_H used and the way to calculate the parameter $\sqrt{J_{2,a}}$. The definition of hydrostatic stress is well established and no

greater difficulty to calculate it exists. The definition of the equivalent shear stress amplitude $\sqrt{J_{2,a}}$ is more complicated. When the applied cyclic loading is uniaxial or in-phase multiaxial, the equivalent shear stress amplitude $\sqrt{J_{2,a}}$ can be determined directly taking the square root of the second invariant of the deviatory tensor:

$$\sqrt{J_{2,a}} = \sqrt{\frac{1}{6}\left\{\left(\sigma_{xx,a}-\sigma_{yy,a}\right)^2+\left(\sigma_{yy,a}-\sigma_{zz,a}\right)^2+\left(\sigma_{zz,a}-\sigma_{xx,a}\right)^2+6.\left(\tau_{xy,a}{}^2+\tau_{yz,a}{}^2+\tau_{xz,a}{}^2\right)\right\}} \tag{7}$$

However, when the applied cyclic loading is out-of-phase multiaxial, the determination of $\sqrt{J_{2,a}}$ is not so simple, requiring complex mathematical calculations. The vector representing the equivalent shear stress amplitude has its direction and magnitude varying along the cycle. Fig. 1(a) shows how the shear stress amplitude varies along the cycle on a proportional and non-proportional loading;

On the point under study, a generic plane Δ can be defined by its unit normal vector n, described by the spherical angles φ and θ, Fig. 1(b). The stress vector Sn acting on a such plane can be decomposed in its normal vector N and the shear stress vector C.

During the load cycle, the tip of the vector Sn describes a closed space curve ψ whose projection on plane Δ is the path of the shear stress vector C on that plane, ψ', Figure 1(c). The shear stress amplitude Ca depends on the orientation of plane Δ, thus Ca = f(φ,θ). To determine the maximum shear stress amplitude Ca,max is necessary to search the maximum of Ca = f(φ,θ) over the angles φ and θ. The critical plane approach requires to find the normal stress and shear stress amplitudes and mean values on each plane Δ passing by the point of interest and then searching the critical plane. For stress invariant approaches, the amplitude of the equivalent shear stress $\sqrt{J_{2,a}}$ remains the same for any orientation of the plane Δ.

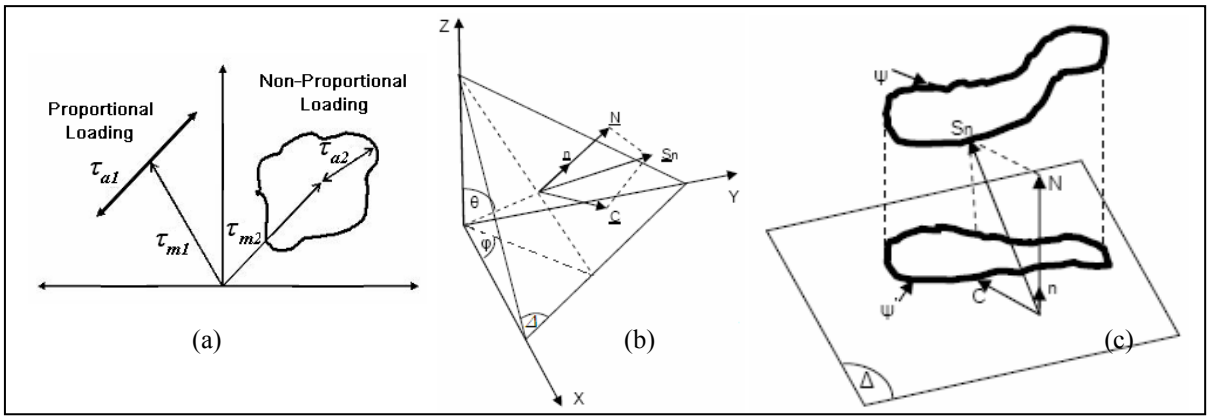

Figure 1 – (a) Behaviour of the shear stress amplitude under proportional and non-proportional loading. (b) Stress vector Sn , normal stress N and shear stress vector C acting on generic plane Δ. (c) Load paths ψ described by the stress vector Sn and ψ' described by the shear stress vector C on a generic plane Δ.

Different methods to calculate the equivalent shear stress amplitude were proposed by Dang Van et al (1988), Deperrois (1991), Duprat et al (1997), Bin Li et al (2000), Mamiya & Araújo (2002) and Balthazar & Malcher (2006).

2.2. The Minimum Simplified Circumscribed Ellipsoid Method

Duprat et al (1997) proposed a method, which could consider the phase angle in tension-bending and torsion stress loading. The model is derived from Crossland criteria, using the projection of the stress tensor path on the deviatory plane. This projection is an ellipse of long axis D and short axis d, Fig. 2. While Crossland original formula uses only D in the calculation of $\sqrt{J_{2a}}$, Duprat et al (1997) replaces D by the half-perimeter of the ellipse, $\frac{p_e}{2}$, to take in account the phase difference, characterized by D and d.

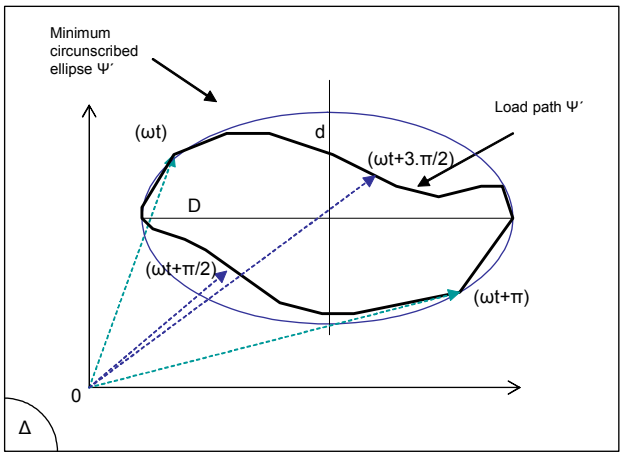

Figure 2: Projection of the tensor path on the deviatory plane.

The values of D and d are given by:

$$D = \max(t)\rho(\omega t)\ ;\ d = \min(t)\rho(\omega t) \tag{8}$$

with the parameter $\rho(\omega t)$ being:

$$\rho(\omega t) = tr\left[\left(\underline{\underline{S}}(t) - \underline{\underline{S}}(t+\pi)\right)\left(\underline{\underline{S}}(t) - \underline{\underline{S}}(t+\pi)\right)\right]^{\frac{1}{2}} \tag{9}$$

where $\underline{\underline{S}}(t)$ is the deviatory stress tensor .

The value of the equivalent shear stress amplitude $\sqrt{J_{2a}}$ is function of the ellipse half-perimeter, $p_e/2$. The perimeter is calculated in function of the parameter D and d, where:

$$\sqrt{J_{2a}} = \frac{1}{2}\cdot\frac{p_e/2}{\sqrt{2}}\ ;\ \frac{p_e}{2} \approx \frac{\pi}{2}\cdot\frac{D+d}{2}\cdot\left[1+\frac{1}{4}\lambda^2+\frac{1}{64}\lambda^4+\frac{1}{256}\lambda^6\right]\ ;\ \lambda = \frac{D-d}{D+d} \tag{10}$$

Balthazar and Malcher (2006) showed the application of this method results in increased scatter for larger phase angles between the applied loads. They showed that a reduction on such scattering could be obtained combining the proposal of Duprat et al (1997) with the minimum circumscribed ellipsoid method proposed by Bin Li et al (2000). The equivalent shear stress amplitude could be calculated as proposed by Bin Li, but using the values of the ellipse semi-axis from the model of Duprat. Thus:

$$\sqrt{J_{2a}} = \sqrt{R_a^2 + R_b^2}\ ;\ R_a = \frac{D}{2} = \frac{\max(t)\rho(\omega t)}{2}\ ;\ R_b = \frac{d}{2} = \frac{\min(t)\rho(\omega t)}{2} \tag{11}$$

The equivalent shear stress amplitude would be then given by:

$$\sqrt{J_{2a}} = \frac{1}{2}\frac{\sqrt{\left[\max(t)\rho(\omega t)\right]^2 + \left[\min(t)\rho(\omega t)\right]^2}}{\sqrt{2}} \tag{12}$$

The main advantage of this modification is the simplicity added to the equivalent shear stress amplitude calculations, as it is easier to determine the ellipse semi-axis D/2 and d/2 as proposed by Duprat than the complex calculations required to obtain the center of the minimum circumscribed hyperesphere or ellipsoid, necessary for the methods of Dang Van, Papadopoulos and Bin Li. Thus, the criterion for multiaxial fatigue can be expressed as:

$$\frac{1}{2}\frac{\sqrt{\left[\max(t)\rho(\omega t)\right]^2 + \left[\min(t)\rho(\omega t)\right]^2}}{\sqrt{2}} + \frac{\sqrt{3}}{S_{rt}}.f_{-1}.\sigma_{H,\max} \le t_{-1} \tag{13}$$

3. RESULTS

Experimental data obtained in the literature were used to assess the different criteria based on the invariant stress approach. It was used 73 results from biaxial constant amplitude loading, from in-phase and out-of-phase tests conducted by Simbürger, 1975 on XC48 steel (group: 100 – test: beding+torsion); by Heidenreich, Richter and Zenner, 1984 on 34Cr4 steel (group: 200 – teste: traction+torsion); by Froustey and Lasserre, 1988 on 30NCD16 (group: 300 – test: beding+torsion) and by Dubar, 1992 on 30NCD16 (group: 400 – test: Beding+torsion) as reported by Weber(1999).

Defining the equivalent stress σ_{eq} to the fully reversed torsional fatigue limit t_{-1} ratio as $K = \sigma_{eq} / t_{-1}$, it is possible to assess the quality the predictions made by each model. If K=1 the model predict perfectly the multiaxial fatigue behaviour. If K is higher than 1, the predictions are conservative. An index of error I can be also established as $I = (K-1)\times 100$.

Tables 1 to 4 and figure 3 show the values of $\sigma_{H,\max}$, $\sqrt{J_{2a}}$, σ_{eq}, I and K for Malcher and Balthazar model. It can be observed that the maximum error lies around 17% on XC48 steel, 7% on 34Cr4 steel, 22% on 30NCD16 steel and 14% on 30NCD16 steel when the phase angle between the applied loads is 90º.

Table 1 – XC48 steel ($t_{-1} = 275MPa$, $f_{-1} = 463MPa$)

Group	Test	Steel	σ11m	σ11a	σ12m	σ12a	α12	Malcher&Balthazar σHmax	√J2a	σeq	K	I
100	101	XC48	0	0	261	261	0	0	261	261	0,95	-5,1
100	102	XC48	0	364	0	209	0	121	296	302	1,10	10,0
100	103	XC48	0	332	0	191	30	111	271	276	1,00	0,4
100	104	XC48	0	315	0	181	60	105	257	262	0,95	-4,8
100	105	XC48	0	328	0	189	90	109	268	273	0,99	-0,7
100	106	XC48	300	300	0	173	0	200	245	255	0,93	-7,4
100	107	XC48	268	268	0	154	90	179	218	227	0,83	-17,4
100	108	XC48	0	319	183	183	0	106	260	265	0,96	-3,7
100	109	XC48	0	294	169	169	90	98	240	244	0,89	-11,1

Table 2 – 34Cr4 steel ($t_{-1} = 256MPa$, $f_{-1} = 410MPa$)

Group	Test	Steel	σ11m	σ11a	σ12m	σ12a	α12	Malcher&Balthazar σHmax	√J2a	σeq	K	I
200	201	34Cr4	0	314	0	157	0	105	240	255	0,99	-0,6
200	202	34Cr4	0	218	0	218	0	73	252	262	1,02	2,3
200	203	34Cr4	0	122	0	244	0	41	254	260	1,01	1,5
200	204	34Cr4	0	382	0	95	0	127	240	258	1,01	0,8
200	205	34Cr4	0	315	0	158	60	105	241	256	1,00	-0,1
200	206	34Cr4	0	316	0	158	90	105	241	256	1,00	0,1
200	207	34Cr4	0	315	0	158	120	105	241	256	1,00	-0,1
200	208	34Cr4	0	224	0	224	90	75	259	269	1,05	5,2
200	209	34Cr4	0	380	0	95	90	127	239	257	1,00	0,4
200	210	34Cr4	0	316	158	158	0	105	241	256	1,00	0,1
200	211	34Cr4	0	314	157	157	60	105	240	255	0,99	-0,6
200	212	34Cr4	0	315	158	158	90	105	241	256	1,00	-0,1
200	213	34Cr4	279	279	0	140	0	186	213	240	0,94	-6,4
200	214	34Cr4	284	284	0	142	90	189	217	244	0,95	-4,8
200	215	34Cr4	0	355	178	89	0	118	223	240	0,94	-6,2
200	216	34Cr4	212	212	0	212	90	141	245	265	1,03	3,4
200	217	34Cr4	0	129	0	258	90	43	269	275	1,07	7,3

Table 3 – 30NCD16 steel ($t_{-1} = 415MPa$, $f_{-1} = 695MPa$)

Group	Test	Steel	σ11m	σ11a	σ12m	σ12a	α12	Malcher&Balthazar σHmax	√J2a	σeq	K	I
300	301	30NCD16	0	485	0	280	0		396	406	0,98	-2,3
300	302	30NCD16	300	630	0	0	0		364	382	0,92	-7,9
300	303	30NCD16	450	550	0	0	0	333	318	337	0,81	-18,7
300	304	30NCD16	510	525	0	0	0	345	303	324	0,78	-22,0
300	305	30NCD16	600	535	0	0	0	378	309	331	0,80	-20,2
300	306	30NCD16	0	480	0	277	90	160	392	401	0,97	-3,3
300	307	30NCD16	300	0	0	395	0		395	401	0,97	-3,4
300	308	30NCD16	300	211	0	365	0		385	395	0,95	-4,8
300	309	30NCD16	300	222	0	385	90		406	416	1,00	0,3
300	310	30NCD16	300	480	0	277	0		392	407	0,98	-1,9
300	311	30NCD16	300	480	0	277	45		392	407	0,98	-1,9
300	312	30NCD16	300	470	0	271	60	257	384	399	0,96	-3,9
300	313	30NCD16	300	473	0	273	90	258	386	401	0,97	-3,3
300	314	30NCD16	300	590	0	148	0		371	389	0,94	-6,3
300	315	30NCD16	300	565	0	141	45	288	355	372	0,90	-10,3
300	316	30NCD16	300	540	0	135	90	280	340	356	0,86	-14,1
300	317	30NCD16	300	455	200	263	0		372	387	0,93	-6,8
300	318	30NCD16	300	465	200	269	90	255	380	395	0,95	-4,8
300	319	30NCD16	450	0	0	395	0		395	404	0,97	-2,7
300	320	30NCD16	450	415	0	240	0	288	339	356	0,86	-14,2
300	321	30NCD16	450	405	0	234	90	285	331	348	0,84	-16,2
300	322	30NCD16	600	0	0	350	0	200	350	362	0,87	-12,8
300	323	30NCD16	600	370	0	214	0	323	302	322	0,77	-22,5
300	324	30NCD16	600	390	0	225	90	330	318	338	0,81	-18,6

Table 4 – 30NCD16 steel ($t_{-1} = 428MPa$, $f_{-1} = 690MPa$)

Group	Test	Steel	σ11m	σ11a	σ12m	σ12a	α12	Malcher&Balthazar σHmax	√J2a	σeq	K	I
400	401	30NCD16	274	624	0	0	0		360	399	0,93	-6,8
400	402	30NCD16	442	588	0	0	0	343	339	384	0,90	-10,4
400	403	30NCD16	603	580	0	0	0	394	335	386	0,90	-9,9
400	404	30NCD16	299	0	0	396	0		396	409	0,96	-4,5
400	405	30NCD16	486	0	0	411	0		411	432	1,01	0,9
400	406	30NCD16	655	0	0	364	0		364	392	0,92	-8,4
400	407	30NCD16	0	482	0	268	0		386	407	0,95	-4,9
400	408	30NCD16	299	207	0	350	0		370	392	0,91	-8,5
400	409	30NCD16	294	474	0	265	0		381	414	0,97	-3,3
400	410	30NCD16	281	584	0	142	0		366	403	0,94	-5,8
400	411	30NCD16	473	447	0	252	0		361	400	0,94	-6,5
400	412	30NCD16	635	425	0	223	0	353	332	377	0,88	-11,9
400	413	30NCD16	0	474	0	265	90	158	381	401	0,94	-6,2
400	414	30NCD16	299	220	0	368	90		389	412	0,96	-3,8
400	415	30NCD16	299	470	0	261	90	256	377	410	0,96	-4,3
400	416	30NCD16	287	527	0	129	90	271	330	365	0,85	-14,6
400	417	30NCD16	472	433	0	240	90	302	347	385	0,90	-10,0
400	418	30NCD16	622	418	0	234	90	347	336	381	0,89	-11,0
400	419	30NCD16	294	451	191	250	0		361	393	0,92	-8,2
400	420	30NCD16	294	462	191	250	90	252	366	398	0,93	-7,0
400	421	30NCD16	294	474	0	265	45	256	381	414	0,97	-3,3
400	422	30NCD16	294	464	0	259	60	253	373	405	0,95	-5,3
400	423	30NCD16	287	554	0	135	45	280	347	383	0,90	-10,5

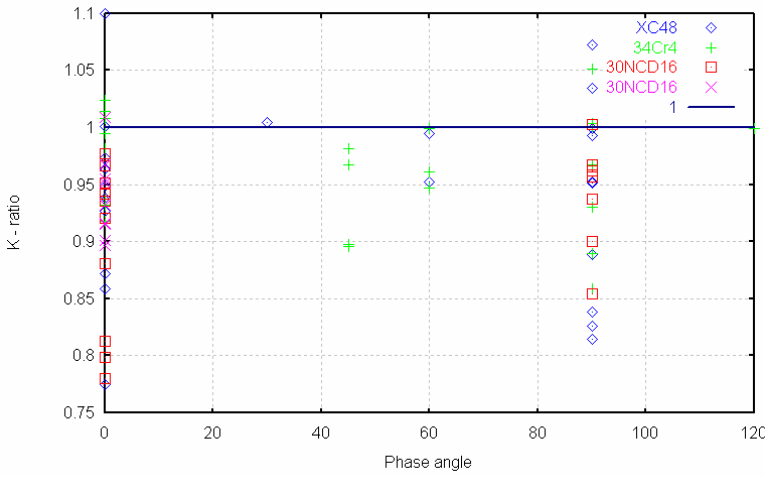

Figure 3: Behaviour of the stress ratio $K = \sigma_{eq} / t_{-1}$ for Malcher & Balthazar model.

Tables 5 to 8 show the values of the index of error I for some models. The models of Bin Li et al, Papadopoulos, Deperrois, Mamiya & Araújo, Marin, Sines, Crossland, Kakuna & Kawada and Balthazar & Malcher were analysed.

Table 5 - Behaviour of the index of error, XC48 steel.
[w]Deperrois;[x]Marin;[y]Papadopoulos;[z]Sines;[M]Malcher&Balthazar

Group	Test	Steel	α12	I_w	I_x	I_y	I_z	I_M
100	101	XC48	0	10,0	11,0	-6,0	-2,0	-5,1
100	102	XC48	0	13,0	11,0	13,0	11,0	10,0
100	103	XC48	30	5,0	-2,0	0,0	-2,0	0,4
100	104	XC48	60	0,0	-17,0	-22,0	-17,0	-4,8
100	105	XC48	90	7,0	-29,0	-10,0	-29,0	-0,7
100	106	XC48	0	-4,0	-2,0	3,0	2,0	-7,4
100	107	XC48	90	-11,0	-34,0	-17,0	-33,0	-17,4
100	108	XC48	0	-1,0	4,0	-1,0	-3,0	-3,7
100	109	XC48	90	-4,0	-28,0	-19,0	-37,0	-11,1

Table 6 - Behaviour of the index of error, 34Cr4 steel.
[w]Crossland;[x]Bin Li et al;[y]Papadopoulos;[z]Mamiya&Araújo;[M]Malcher&Balthazar

Group	Test	Steel	α12	I_w	I_x	I_y	I_z	I_M
200	201	34Cr4	0	-0,5	-0,6	-0,6	-0,6	-0,6
200	202	34Cr4	0					2,3
200	203	34Cr4	0					1,5
200	204	34Cr4	0					0,8
200	205	34Cr4	60	-12,3	-0,1	-0,1	-0,2	-0,1
200	206	34Cr4	90	-22,7	0,1	0,1	0,1	0,1
200	207	34Cr4	120	-5,1	-0,1	-0,1	-0,2	-0,1
200	208	34Cr4	90	-8,4	5,2	5,2	5,2	5,2
200	209	34Cr4	90	-7,3	0,4	0,4	0,4	0,4
200	210	34Cr4	0	0,5	0,1	0,1	0,1	0,1
200	211	34Cr4	60	-12,3	-0,6	-0,6	-0,6	-0,6
200	212	34Cr4	90	-21,8	-0,2	-0,1	-0,1	-0,1
200	213	34Cr4	0	-6,4	-6,4	-6,4	-6,4	-6,4
200	214	34Cr4	90	-25,5	-4,9	-4,8	-4,8	-4,8
200	215	34Cr4	0					-6,2
200	216	34Cr4	90	-9,4	3,4	3,4	3,4	3,4
200	217	34Cr4	90					7,3

Table 7 - Behaviour of the index of error, 30NCD16 steel.
[w]Crossland;[x]Deperrois;[y]Marin;[z]Papadopoulos;[M]Malcher&Balthazar

Group	Test	Steel	α12	I_w	I_x	I_y	I_z	I_M
300	301	30NCD16	0	-2,0	1,0	-1,0	0,0	-2,3
300	302	30NCD16	0	-8,0	-8,0	-6,0	-2,0	-7,9
300	303	30NCD16	0	-19,0	-19,0	-12,0	-10,0	-18,7
300	304	30NCD16	0	-22,0	-22,0	-13,0	-13,0	-22,0
300	305	30NCD16	0	-20,0	-20,0	-7,0	-9,0	-20,2
300	306	30NCD16	90	-31,0	4,0	-31,0	-12,0	-3,3
300	307	30NCD16	0	-3,0	11,0	2,0	2,0	-3,4
300	308	30NCD16	0	-5,0	6,0	-1,0	3,0	-4,8
300	309	30NCD16	90	-5,0	14,0	-1,0	4,0	0,3
300	310	30NCD16	0	-2,0	1,0	1,0	6,0	-1,9
300	311	30NCD16	45	-9,0	3,0	-6,0	0,0	-1,9
300	312	30NCD16	60	-16,0	1,0	-13,0	-5,0	-3,9
300	313	30NCD16	90	-31,0	4,0	-27,0	-6,0	-3,3
300	314	30NCD16	0	-6,0	-6,0	-4,0	0,0	-6,3
300	315	30NCD16	45	-13,0	-9,0	-11,0	-7,0	-10,3
300	316	30NCD16	90	-21,0	-12,0	-18,0	-11,0	-14,1
300	317	30NCD16	0	-7,0	-4,0	1,0	1,0	-6,8
300	318	30NCD16	90	-32,0	2,0	-22,0	-8,0	-4,8
300	319	30NCD16	0	-3,0	12,0	6,0	5,0	-2,7
300	320	30NCD16	0	-14,0	-11,0	-7,0	-4,0	-14,2
300	321	30NCD16	90	-40,0	-10,0	-30,0	-15,0	-16,2
300	322	30NCD16	0	-13,0	0,0	1,0	-2,0	-12,8
300	323	30NCD16	0	-23,0	-20,0	-9,0	-10,0	-22,5
300	324	30NCD16	90	-41,0	-13,0	-24,0	-14,0	-18,6

Table 8 - Behaviour of the index of error, 30NCD16 steel.
[w]Kakuna&Kawada;[x]Sines;[y]Marin;[z]Papadopoulos;[M]Malcher&Balthazar

Group	Test	Steel	α12	I_w	I_x	I_y	I_z	I_M
400	401	30NCD16	0	1,0	1,0	-7,0	-7,0	-6,8
400	402	30NCD16	0	2,0	2,0	-7,0	-11,0	-10,4
400	403	30NCD16	0	7,0	7,0	-2,0	-10,0	-9,9
400	404	30NCD16	0	4,0	11,0	2,0	-5,0	-4,5
400	405	30NCD16	0	15,0	22,0	11,0	0,0	0,9
400	406	30NCD16	0	10,0	17,0	6,0	-9,0	-8,4
400	407	30NCD16	0	-5,0	-3,0	-3,0	-5,0	-4,9
400	408	30NCD16	0	0,0	4,0	-4,0	-9,0	-8,5
400	409	30NCD16	0	5,0	7,0	-1,0	-4,0	-3,3
400	410	30NCD16	0	2,0	3,0	-5,0	-6,0	-5,8
400	411	30NCD16	0	7,0	9,0	-1,0	-7,0	-6,5
400	412	30NCD16	0	6,0	8,0	-1,0	-12,0	-11,9
400	413	30NCD16	90	-31,0	-31,0	-31,0	-7,0	-6,2
400	414	30NCD16	90	0,0	4,0	-4,0	-4,0	-3,8
400	415	30NCD16	90	-20,0	-20,0	-27,0	-5,0	-4,3
400	416	30NCD16	90	-13,0	-13,0	-20,0	-15,0	-14,6
400	417	30NCD16	90	-19,0	-19,0	-26,0	-10,0	-10,0
400	418	30NCD16	90	-15,0	-15,0	-20,0	-11,0	-11,0
400	419	30NCD16	0	0,0	2,0	-2,0	-9,0	-8,2
400	420	30NCD16	90	-22,0	-22,0	-24,0	-6,0	-7,0
400	421	30NCD16	45	-2,0	0,0	-8,0	-4,0	-3,3
400	422	30NCD16	60	-9,0	-8,0	-15,0	-6,0	-5,3
400	423	30NCD16	45	-5,0	-5,0	-13,0	-11,0	-10,5

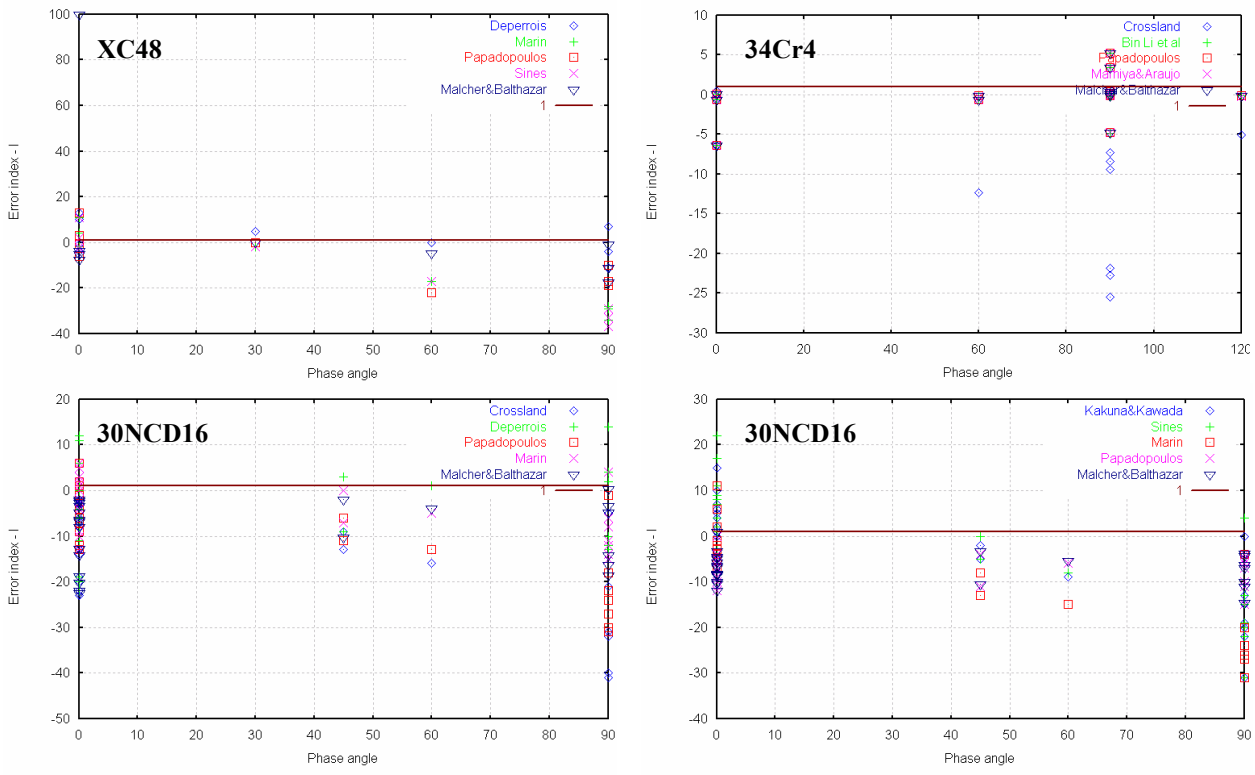

Figure 4: Behaviour of the index of error $I = (K-1)\times 100$ for Bin Li et al, Papadopoulos, Deperrois, Mamiya & Araújo, Marin, Sines, Crossland, Kakuna & Kawada and Balthazar & Malcher models.

4. CONCLUSIONS

A new simplified proposal to calculate the equivalent shear stress amplitude based on the stress invariant method, called The Minimum Simplified Circumscribed Ellipsoid Method which combines the proposal of Duprat et al (1997) with the minimum circumscribed ellipsoid method of Bin Li et al (2000), is proposed. The new method to determine the equivalent shear stress amplitude eliminates the need the complex calculations required by the other methods without losing quality in the results.

Notwithstanding the results given by the present proposal being similar to the results obtained with the other models, the present proposal represents a simplified way to determine the equivalent shear stress amplitude, eliminating the need the complex calculations required by the other methods, without losing quality in the results

The results showed the determination of the equivalent shear stress amplitude considerable reduces the scatter observed withy other models in the literature. For the analysed data the scatter was limited to ± 10%.

5. REFERENCES

BALTHAZAR, J.C., MALCHER, L., A review on the main approaches for determination of the multiaxial high fatigue strength. Solid Mechanics in Brazil 2007. Brazilian Society of Mechanical Sciences and Engineering, 2007, v. 1, p. 63-80;

BIN LI, SANTOS, J.L.T., FREITAS, M., A Unified Numerical Approach for Multiaxial Fatigue Limit Evaluation, Mech. Struct. & Mach., Vol. 28, 1, 2000, p.p. 85-103;

CROSSLAND, B. Effect of large hydrostatic pressures on the torsional fatigue strength of an alloy steel, in: Proc. Int. Conf. on Fatigue of Metals, IMechE, London, 1956, pp. 138–149;

DANG VAN, K., Sur la Résistance à la fatigue des Métaux. Sciencies et Technique de L' armement, 1973, 47, 429-453 ;

DEPERROIS, A., Sur le Calcul de Limites D'Endurance des Aciers, These de Doctorat, Ecole Polytechnique, 1991, Paris ;

DUBAR, L., Fatigue multiaxiale des aciers. Passage de I'endurance à I'endurance limiteé. Prise en compte des accidents géométriques.Thèse de I'ENSAM, Talence, Juin 1992, 165 p ;

DUPRAT, D., BOUDET, R., DAVY, A., A Simple Model to Predict Fatigue Strength with Out-of Phase Tension-Bending and Torsion Stress Condition, Proc. 9th Int. Conf Fracture, Sidney, Australia, 1997, p.p. 1379-1386;

KAKUNO H., KAWADA Y., A New Criterion of Fatigue Strength of a Round Bar Subjected to Combined Static and Repeated bending and Torsion, Fatigue Engng Mat Struct, 1979, Vol. 2, pp. 229-236;
LEMPP, W., Festigkeitsverhalten von stählen bei mehrachsiger dauerschwingbeanspruchung durch normalspannungen mit überlagerten phasengleichen und phasenverschobenen schubspannungen. Diss. TU Stuttgard, 1977;
MALCHER, L. (2006). Um Modelo para Determinação da Resistência à Fadiga Multiaxial para Carregamentos de Flexão e Torção Combinados, Fora de Fase e com Amplitude Constante. Com Base no Critério do Invariante do Tensor. Dissertação de Mestrado, Publicação ENM.DM-105A/06, Departamento de Engenharia Mecânica, Universidade de Brasília,DF, 88 p;
MALCHER, L., BALTHAZAR, J.C., An Analysis of the Ellipsoid Simplified Model for Determination of the Fatigue Strength in Biaxial/Triaxial Loading and Out-of-Phase, Proc.16ºPOSMEC - 16º Simpósio de Pós-Graduação em Engenharia Mecânica, Uberlandia, Brazil, 2006;
MAMIYA, E. N., ARAUJO, J. A., Fatigue Limit Under Multiaxial Loadings: On The Definition of The Equivalent Shear Stress. Mechanics Research Communications, 2002, V29, pp 141-151;
NISHIHARA, T., KAWAMOTO, M., The Strength of metals under combined alternating bending and torsion with phase difference. Memoirs of College of Engineering, Kyoto Imperial University, 1945, Vol. 11, Nº 5, pp. 85-112;
PAPADOPOULOS, I.V. and DANG VAN, K., Sur la Nucleation des Fissures en Fatigue Polycyclique sous Chargement Multiaxial, Arch. Mech., Vol. 40, 1988, p.p. 759-774
PAPADOPOULOS, I. V., A review of multiaxial fatigue limit criteria . ECJRC, SMU, Ispra, (Va), 1992 ;
SIMBÜGER, A., Festigkeitsverhalten zäher werkstoffe bei einer mehrachsigen phasenverschobenen schwingbeanspruchug mit körperfesten und veränderlichen hauptspannungrichtungen. L.B.F., Darmstadt, Bericht, 1975, Nr.FB-121,247 p;
SINES, G., Failure of materials under combined repeated stresses with superimposed static stresses, NACA Technical Note 3495, Washington, USA, 1955;
WEBER, B., Fatigue multiaxiale des structures industrielles sous chargement quelconque. Thèse de Ingénieur de I'Institut National des Sciences Appliquées de Lyon, 1999, 247 p ;

6. RESPONSIBILITY NOTICE

The authors are the only responsible for the printed material included in this paper.